 doi:10.20944/preprints202211.0069.v1

Article

Cell/Tissue based Reconstituted Lipid Nanoparticles as Versatile Drug Delivery Carrier

Cheng Wang[1,*]

[1] School of Pharmacy, Changzhou University, Changzhou, Jiangsu 213164, P. R. China.
* Correspondence: Corresponding author: Cheng Wang, wangc90@cczu.edu.cn

Abstract: Nanomedicine holds great potential to devise better drug delivery systems (DDSs). However, many reported nanomedicines still fall short of commercial requirements including specific targetability, scale-up manufacturing and safety. Cell/tissue based carriers, including cell membrane vehicle and exosome, are biocompatible and targeting platforms but usually suffered from low yields and unstable reproducibility. Here in this study, we proposed the concept and preparation of reconstituted lipid nanoparticles (rLNPs) to develop highly reproducible cell/tissue based lipid nanoparticles (LNPs) for drug delivery, which holds the potential as a versatile drug delivery platform. The whole lipids of cell or tissue were firstly extracted and then prepared into rLNPs using solvent diffusion method. In this way, the preparation of ultra-small (~20 nm) rLNPs can be easily applied to both cell (mouse breast cancer cell line, 4T1) and tissue (mouse liver tissue). Our results demonstrated that mouse liver tissue derived rLNPs can be further labeled/modified with imaging, targeting or other functional moieties. Furthermore, rLNPs were highly biocompatible and capable of loading different drugs including doxorubicin hydrochloride (Dox) and curcumin (Cur). Most importantly, Dox loaded rLNPs (rLNPs/Dox) showed preferable in vitro and in vivo anticancer performance. Therefore, rLNPs might be a versatile drug delivery platform for future application in the treatment of a variety of diseases.

Keywords: reconstituted lipid nanoparticles; drug delivery systems; solvent diffusion method

1. Introduction

In recent decades, nanomedicine, as an interdisciplinary field that integrates nanoscience and nanotechnology with life science, has become one of the most productive research fields across the globe, [1, 2] with many fruitful results achieved in laboratory and clinical applications. [3, 4] The related research in nanomedicine spans multiple areas, including drug delivery, vaccine formulation, wearable devices, etc., [5] and has versatile functionalities ranging from diagnosis to disease treatments. [6] In particular, for drug delivery, many previous studies have confirmed that nanomedicine can significantly increase the bioavailability and safety of free drugs, which can offer enhanced therapeutic performance. [7-9] Therefore, it is expected that nanomedicine will lead to the development of better drug delivery systems (DDSs) for the treatment of a wide range of diseases with high specificity, efficacy, and personalization. [10]

The key to successful DDSs is to find suitable carriers. [11] Currently, the reported carriers are of various types, such as micelles and liposomes, [12, 13] and they are composed of diverse materials, including both organic and inorganic materials derived from natural or artificial sources. [14, 15] Despite their promising results, current DDSs still face extensive challenges, such as 1) passing through biological barriers and achieving specific targeting; 2) scale-up manufacturing; and 3) pharmacology and safety concerns. [16] Due to these obstacles, although various drug delivery carriers have been produced by scientists for several decades, so far, only a handful of products have overcome these challenges and become commercially available. For example, in cancer nanomedicine, only 14 systemically administered products have been approved worldwide for clinical use. [17]

 doi:10.20944/preprints202211.0069.v1

In recent years, cell/tissue-based carriers, such as cell membrane vehicles and exosomes, have gained increasing attention. [18, 19] They are constituted by a part of the cell/tissue and therefore can avoid safety issues, such as immunogenicity and cytotoxicity. [20] They can also be tailored by selecting a specific progenitor cell type or using a fusing technique to successfully overcome the challenges of biological barriers to realize specific targeting. [21] Although these DDSs usually have low yields and unstable reproducibility, which fail to meet the scale-up manufacturing requirements for clinical applications, they still represent an appropriate strategy to develop biocompatible carriers for better drug delivery that inspired us to find other new ways to develop cell/tissue-based drug carriers.

Lipid nanoparticles (LNPs), including solid lipid nanoparticles (SLNs), nanostructured lipid carriers (NLCs), and liposomes, are generally regarded as nontoxic, biocompatible, and easy-to-produce formulations. [22, 23] Hu et al. proposed a facile solvent diffusion method to prepare LNPs by simply injecting the organic phase of lipids into water, which shows high accessibility and reproducibility and may pave the way for mass production. [24] Moreover, previous studies have demonstrated that finely tuned LNPs showed high applicability for *in vivo* applications and could overcome the challenges of biological barriers for specific targeting. [25, 26] Therefore, LNPs might be one of the most suitable platforms for clinical drug delivery, as most of the currently available commercial formulations are based on LNPs. [17, 22]

Enlightened by the previous research described above, in this study, with the aim of developing convenient and highly reproducible cell/tissue-derived LNPs for drug delivery, the author proposed the concept and preparation of reconstituted lipid nanoparticles (rLNPs). In detail, the whole lipids of cells or tissue were first extracted using an established method [27] and then prepared into rLNPs using a solvent diffusion method. In this way, the rLNPs can be easily applied to different cells or tissues. Moreover, the rLNPs can either be labeled with fluorescent molecules or modified by targeting ligands and other functional moieties to equip them with imaging, cell/tissue targeting, or other functions. In this study, 4T1 cells (a mouse breast cancer cell line) and mouse liver tissue-derived rLNPs were successfully constructed and characterized. Afterward, mouse liver tissue-derived rLNPs were selected as the model carrier for fluorescence labeling/targeting ligand modification, drug loading and biocompatibility and *in vivo* orthotopic 4T1 tumor accumulation assays. Finally, the *in vitro* and *in vivo* anticancer efficacy of doxorubicin hydrochloride (Dox)-loaded rLNPs (rLNP/Dox) was tested using 4T1 cells and an orthotopic 4T1 tumor model.

2. Materials and methods

2.1. Materials

Doxorubicin hydrochloride (Dox), curcumin (Cur), coumarin 6 (C6), indocyanine green (ICG), and methyl thiazolyl tetrazolium (MTT) were purchased from Aladdin (Shanghai, China). DSPE-PEG_{2000}-Biotin was offered by AVT Pharmaceutical Tech Co., Ltd., (Shanghai, China). All other chemicals without specific statements were from Aladdin and of analytical pure.

2.2. Preparation of rLNPs

The extraction of full lipids from cells and tissues followed the protocol of previous report with some modifications. [27] In brief, 100 mg of fresh tissue (or 5 ×10^7 cells) was cut into pieces and loaded into a glass homogenizer with 500 μL of 75% methanol. After grinding about 50 times at 0 ℃, the mixture was transferred to a brown test tube containing another 1 mL of methyl-*tert*-butyl ether (MTBE). The tube was placed in a shaker for 1 h to allow the full extraction of lipids. Afterward, 250 μL of pure water was added into the tube and the mixture was allowed to stay for 10 min for phase separation and followed

 doi:10.20944/preprints202211.0069.v1

by centrifugation at 14000 rpm for 15 min at 0 ℃. The upper MTBE phase with concentrated lipids was transferred to another new brown test tube and dried using a nitrogen-blowing instrument.

The obtained lipids were dissolved in ethanol to achieve designated concentrations. Afterward, the solvent diffusion method was applied by injecting the ethanol solution into pure water (volume ratio of 1: 9) at a constant rate (0.1 mL/s) via syringe under agitation (500 rpm) according to the author's previous study. [28]

2.3. Characterization of nanoparticles

The size and zeta potential of nanoparticles were assessed using a Size-Zeta analyzer (Litesizer 500, Anton Paar, Austria). The morphology of nanoparticles was observed using transmission electron microscopy (TEM, HT-7800, Hitachi, Japan).

2.4. Drug loading, in vitro drug release, and surface modification

The Dox and Cur were dissolved in ethanol solution with the extracted lipids and then injected into pure water as mentioned above to prepare drug-loaded rLNPs.

For fluorescence labeling, C6 was dissolved in ethanol solution (0.5%) with the extracted lipids and then injected into pure water as mentioned above. For targeting ligand modification, DSPE-PEG_{2000}-Biotin (10% weight ratio of total lipids) was dissolved in ethanol solution with the extracted lipids and then injected into pure water as mentioned above.

The unloaded drugs or molecules were removed by filtration through a 0.22 μm membrane (Millipore, USA) followed by dialysis against water (MWCO: 3500 Da). The UV-vis spectrum of rLNPs, free drugs and drug-loaded rLNPs was recorded using UV-vis spectrophotometer.

2.5. Cell culture, multi-cellular tumor spheroid (MCTS) and animal models

4T1 (mouse breast cancer cell line) and NIH3T3 (mouse embryonic fibroblast) cells were obtained from Shanghai Zhong Qiao Xin Zhou Biotechnology Co., Ltd (Shanghai, China). Cells were cultured in RPMI-1640 medium supplied with 10% fetal bovine serum (FBS, Gibco, USA) and placed in an incubator (Forma Direct Heat, Thermo Scientific, USA) at a temperature of 37 ℃ and atmosphere of 95% air/5% CO_2. Cells in the logarithmic phase were employed for experiments.

The MCTS model was established according to the previous report. [29] In brief, a 96-well plate (Corning, USA) was individually covered with 50 μL of autoclaved agarose solution (2 %, w/v) to give a gel matrix with concavity. Afterward, equally mixed 4T1 and NIH3T3 cells were seeded at a total density of 2×10^3 cells/well and cultured in standard conditions for 3-4 days to give MCTS.

Balb/c mice (female, 6-8 weak) were offered by Cavens animal center (Changzhou, China) and housed in SPF conditions with free access to food and water. The mice were subcutaneously injected with 50 μL of 4T1 cell suspension (4×10^7 cells/mL) to the mammary gland. All subjects were returned to above-mentioned feeding condition for the establishment of orthotopic 4T1 tumor-bearing mouse model. All animal experiments were approved by the Animal Care and Use Committee of Changzhou University in accordance with the guidelines for the care and use of laboratory animals.

2.6. Cellular uptake

4T1 cells were seeded in 24 well plates at the density of 5×10^4 cells/well and allowed to grow overnight. Afterward, the primary medium was removed and replaced with a fresh FBS-free medium containing C6 labeled rLNPs or C6/Biotin dual modified rLNPs (nanoparticle concentration:100 μg/mL) and continued to incubate for different time intervals (3, 6, 12 h). At designated time points, cells were fixed with 4% paraformaldehyde

 doi:10.20944/preprints202211.0069.v1

(15 min). Samples were observed and imaged under an inverted fluorescence microscope (Ti2, Nikon, Japan).

2.7. Biocompatibility assay

The biocompatibility of rLNPs was assessed according to the previous report. [30] In brief, for hemolysis assay, different concentrations of rLNPs were incubated with 2% red blood cells (from New Zealand rabbit, Hongquan Bio, Guangzhou, China) suspension at 37 °C for 1 h. The measurement of hemoglobin leakage was performed by recording UV-vis absorbance at 545 nm. For cytotoxicity, 4T1 and NIH3T3 cells in 96-well plates (3×10^3 cells/well for overnight incubation) were replaced with serum-free medium containing rLNPs at designated concentrations (20, 50, 100, 150, 200 μg/mL) for another 24 h of incubation, followed by cell viability measurement using MTT assay. For systemic toxicity, Balb/c mice were randomly divided into 2 groups (n=3) and administered with saline (control) and rLNPs (100 mg/kg) every other day for 14 days via tail vein injection. The body weights of all subjects were recorded before each injection. At last, mice were sacrificed and the obtained main organs were subjected to HE analysis.

2.8. In vivo tumor accumulation and bio-distribution

To reveal the *in vivo* tumor accumulation capacity of rLNPs, indocyanine green (ICG) was employed to label rLNP using the above-mentioned protocol. Subsequently, ICG labeled rLNPs were intravenously injected into the orthotopic 4T1 tumor-bearing mice (n=3). At prearranged time intervals (6, 24, and 48 h), the distribution of fluorescence signal within the mice was recorded at an excitation wavelength of 790 nm and an emission wavelength of 845 nm using the *in vivo* imaging system (IVIS Lumina Series III, PerkinElmer, USA). After living imaging, one mouse was sacrificed, and the main organs and tumor tissues were excised for *ex vivo* imaging using the same imaging system.

2.9. Therapeutic performance

2.9.1. In vitro anticancer effect

The *in vitro* anticancer effect of rLNPs/Dox was assessed. In brief, 4T1 cells in 96-well plates were incubated with serum-free medium containing free Dox or rLNPs/Dox at designated concentrations (0.1, 0.5, 1, 2, 5 μg/mL) for 24 h, followed by cell viability measurement using MTT assay. Additionally, MCTSs with diameter of 200-300 μm were incubated with a fresh medium containing free Dox or rLNPs/Dox (Dox concentration: 1 μg/mL) at 37 °C for 4 days. The diameter of the MCTSs was recorded every day using an optical microscope (Primovert iLED, Zeiss, Germany) with untreated MCTS as control.

2.9.2. In vivo anticancer effect

Orthotopic 4T1 tumor-bearing mice with a tumor volume around 100 mm^3 were divided into three groups (n=3) and treated with saline, free Dox, rLNPs, or rLNPs/Dox (Dox dosage: 5 mg/kg) every other day for 14 days. The tumor volumes of all subjects were recorded before drug administration. The mice were sacrificed at the end of the test and the tumor tissues of the subjects were obtained for physiopathological analysis using HE and Ki67 staining.

3. Results and discussion

3.1. The preparation of rLNPs is highly reproducible using extracted lipids from both cells and tissue

In this study, rLNPs were prepared by sequential steps, including lipid extraction and nanoparticle preparation. To explore whether this method can be equally applied to cells and tissue, 4T1 cells and mouse liver tissue were selected as representative models. As shown in Figure 1, using the same protocol, both 4T1 cells and mouse liver tissue can

 doi:10.20944/preprints202211.0069.v1

be prepared into nanoscale particles with a size of approximately 20 nm (Figure 1A and B). The TEM images revealed that the as-prepared rLNPs were near-spherical particles with good dispersion (Figure 1C and D), and the major size distribution was located at approximately 20 nm. These results demonstrated that the proposed method is a robust way to prepare rLNPs with high reproducibility. Therefore, due to the high accessibility of organs, mouse liver-derived rLNPs were selected as the model carrier in the following studies unless otherwise stated.

In addition, previous studies have indicated that under certain charge ratios, NLCs composed of different types of lipids can have smaller sizes, more regular morphology in a spherical shape, and improved dispersity than SLNs with a single solid lipid. [24, 31] In this regard, the rLNPs prepared in this study can be regarded as a novel kind of NLC. Previous study revealed that NLCs prepared using phospholipids as the major component can reach a small size of approximately 20 nm. [28] As phospholipids are the major lipid component of cells, the results not only further confirm the conclusion of this previous study but also suggest that NLCs with phospholipids as the major component may allow for the preparation of nanoparticles with ultrasmall sizes, which can be used in drug delivery applications with strict size requirements.

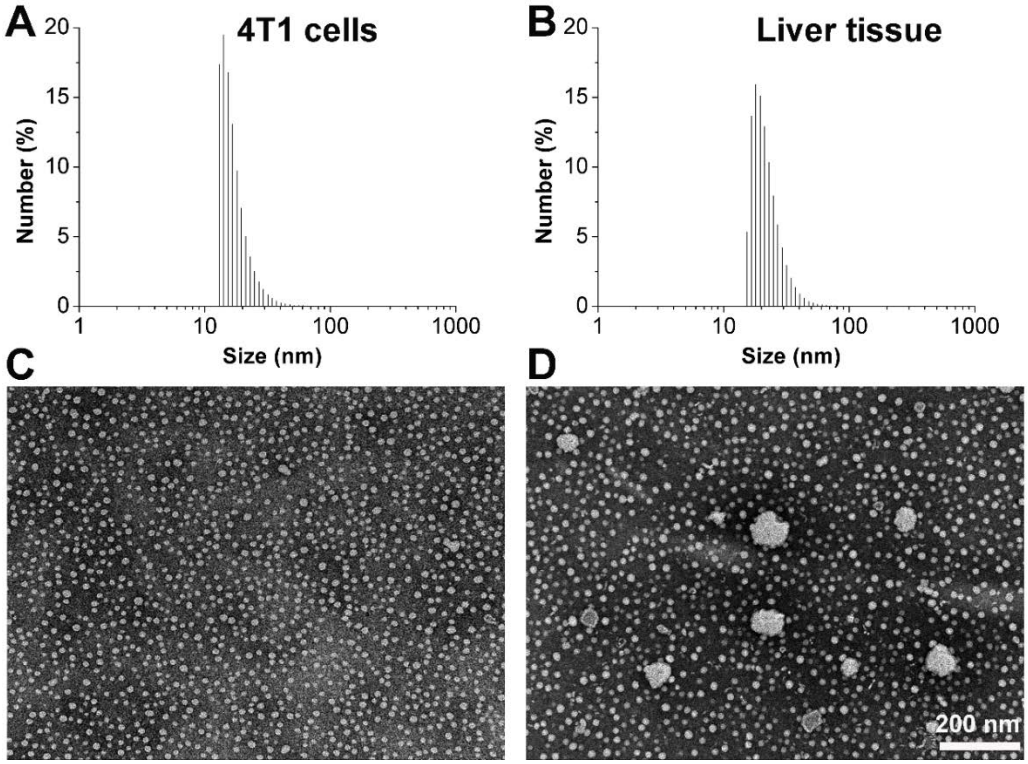

Figure 1. Size distribution (A and B) and morphology observation (C and D) of rLNPs prepared using lipids extracted from 4T1 cells and mouse liver tissue. Scale bar: 200 nm.

3.2. The fluorescence labeling and ligand modification of rLNPs can be readily realized

The fluorescence labeling and ligand modification of rLNPs were also studied. C6 was first employed for fluorescence labeling of rLNPs. The successful modification was verified by monitoring the fluorescence signals in 4T1 cells. As shown in Figure 2, C6 labeling can be utilized to reflect the cellular uptake profile of rLNPs. Similar to similar studies, the as-prepared rLNPs also showed time-dependent cellular uptake by 4T1 cells, with the fluorescence signal increasing over time. [32, 33] Afterward, the rLNPs were further modified with DSPE-PEG_{2000}-Biotin to provide a targeting ligand (biotin), and 4T1 cells overexpressing the biotin receptor [34] were selected as a model. Compared with unmodified rLNPs, biotin modification resulted in a significant increase in rLNP uptake

Preprints (www.preprints.org) | NOT PEER-REVIEWED | Posted: 3 November 2022 doi:10.20944/preprints202211.0069.v1

by 4T1 cells under all tested intervals, which suggested the successful functionalization of rLNPs using targeting ligands. These results suggested that rLNPs possess the flexible labeling and modification aspects of traditional LNPs, which can be an indispensable advantage for their future applications in other fields.

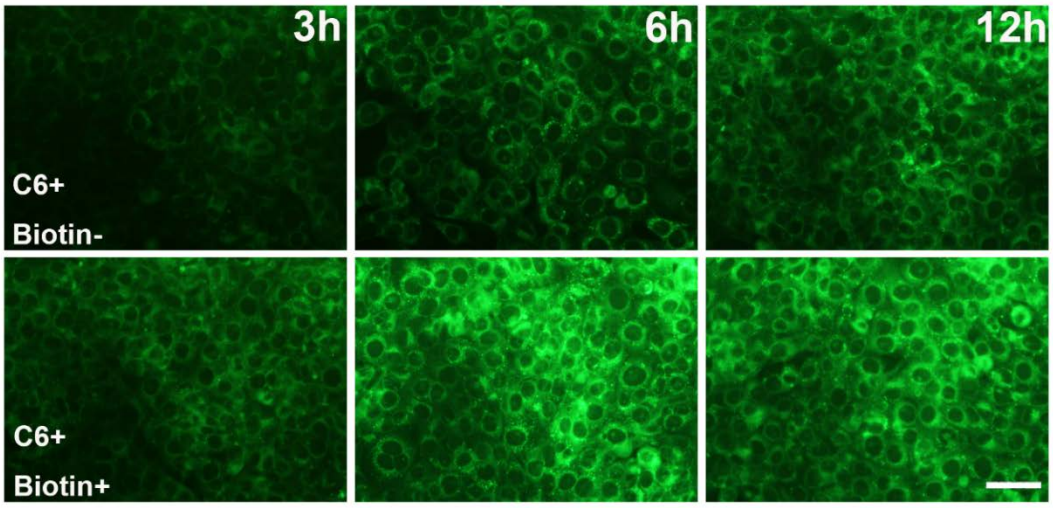

Figure 2. Time-dependent cellular uptake profile of unmodified (upper channels) and biotin-modified (lower channels) C6-labeled rLNPs in 4T1 cells. Scale bar: 50 μm.

3.3. The rLNPs show high biocompatibility

To explore the safety profile of rLNPs, the hemolysis potential of different concentrations of rLNPs was tested. As shown in Figure 3A, rLNPs showed almost no hemolysis risk on red blood cells under all given concentrations, with only 1.39% at the highest concentration of 2 mg/mL. Therefore, rLNPs are believed to exert no hemolysis risk upon *in vivo* application. The *in vitro* cytotoxicity of rLNPs against both 4T1 and 3T3 cells was also studied. Moreover, healthy mice were intravenously administered an extremely high dose of rLNPs (100 mg/kg) every 2 days for 14 days. The body weight variations and organ pathological changes of the subjects were studied to evaluate the biocompatibility of the rLNPs. As shown in Figure 3B, the body weight of all recipients during the test showed no insignificant differences between the rLNPs and control groups, which suggested that the health of mice subjected to high-dose rLNPs was not affected. This conclusion was also supported by the HE staining results of major organs after administration. As shown in Figure 3C, no apparent pathological changes were observed in the major organs of the rLNP group. These results jointly suggest that the as-prepared rLNPs are highly biocompatible carriers for *in vivo* applications.

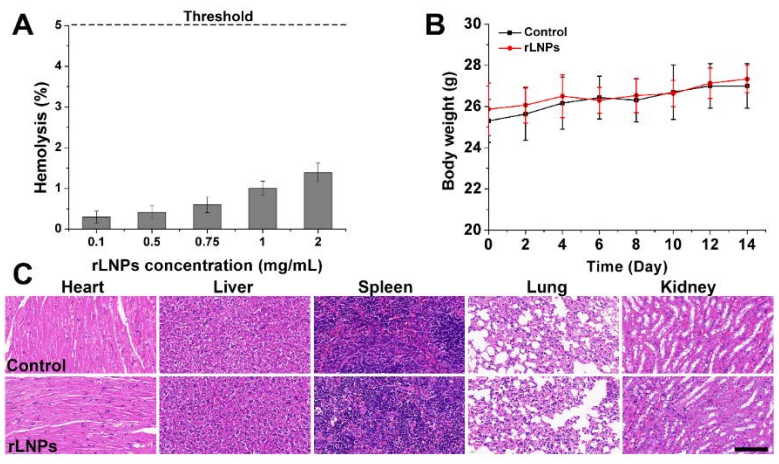

Preprints (www.preprints.org) | NOT PEER-REVIEWED | Posted: 3 November 2022 doi:10.20944/preprints202211.0069.v1

Figure 3. Biocompatibility assays of rLNPs. (A) Hemolysis of 2% red blood cells after treatment with various concentrations of rLNPs for 1 h. (B) Body weight variations of mice intravenously administered rLNPs (100 mg/kg) every other day for 14 days. Data are shown as the mean values and standard deviations of three independent results. (C) HE histopathological sections prepared from major organs that were harvested from the recipients at the end of the administration. Scale bar: 100 μm.

3.4. The rLNPs show preferable tumor accumulation and long-circulation properties

Next, the author aimed to explore the tumor accumulation ability of rLNP, which is critical in cancer therapy. ICG as a near-infrared probe was used to label the rLNPs using a similar protocol for fluorescence labeling. After intravenous injection of ICG-labeled rLNPs for different time intervals, the ICG signal within the subjects was visualized to indicate the distribution of the rLNPs. As shown in Figure 4, rLNPs showed observable accumulation in the tumor 6 h after injection and gradually accumulated to a higher level with increasing time. In particular, as supported by *in vivo* (Figure 4C) and *ex vivo* imaging (Figure 4D), even 48 h after injection, the retention of rLNPs in the tumor tissue was still more prominent than in the major organs, which suggested their good accumulation and retention potential in tumor tissue.

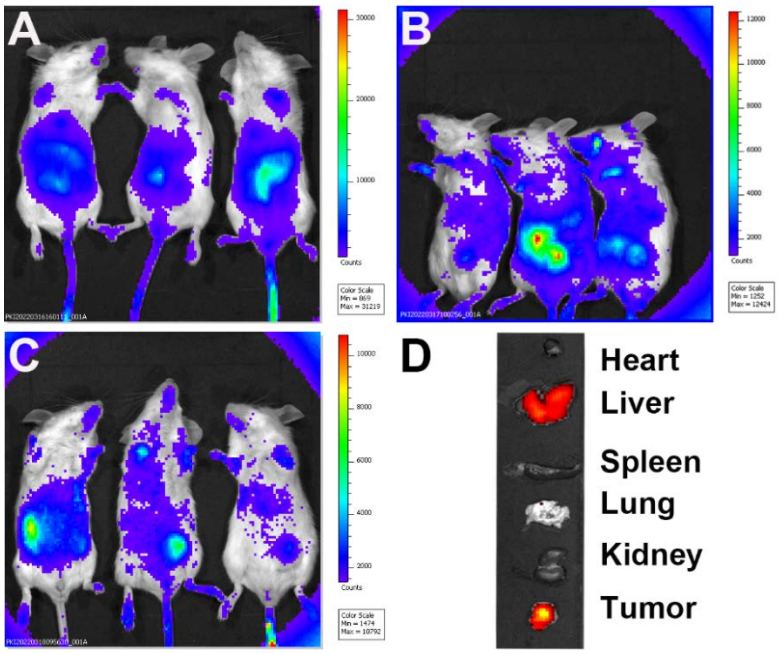

Figure 4. *In vivo* tumor accumulation assay of rLNPs. ICG-labeled rLNPs were intravenously injected into orthotopic 4T1 tumor-bearing mice, and the distribution of ICG signals within the subjects at 6 (A), 24 (B), and 48 h (C) was visualized by live imaging. At 48 h postinjection, the main organs and tumor tissues of one subject were excised for *ex vivo* imaging (D).

3.5. The rLNPs can be loaded with different types of drugs

The different lipids in NLCs can offer spatial imperfection and an unstructured crystal structure within their lipid matrix, which provide space for higher drug accommodation. [35] The prepared rLNPs were composed of various lipid components from the parent cell/tissue that were expected to possess the drug loading capacity of NLCs. Therefore, Dox as a hydrophilic drug and Cur as a hydrophobic drug were selected to explore the drug loading potential of the rLNPs. As shown in Figure 5A, the UV–vis spectrum revealed that rLNPs/Dox retained the characteristic peak of Dox at approximately 480 nm, which suggested the successful loading of Dox into the rLNPs. Similar to a previous report, as a hydrophilic drug Dox was loaded into the lipid matrix of rLNPs, possibly due to ion-pair formation with the negatively charged lipid components. [36] The TEM image in Figure 5C revealed that rLNPs/Dox had a near-spherical shape with a slightly increased

 doi:10.20944/preprints202211.0069.v1

size and good dispersion. Moreover, the results in Figures 5B and D also confirmed the successful loading of Cur into rLNPs, and the obtained rLNPs/Cur was also well dispersed as a DDS. These results suggested the capability of rLNPs for the loading of different drugs and demonstrated their potential to be applied as a drug carrier for the delivery of other drugs.

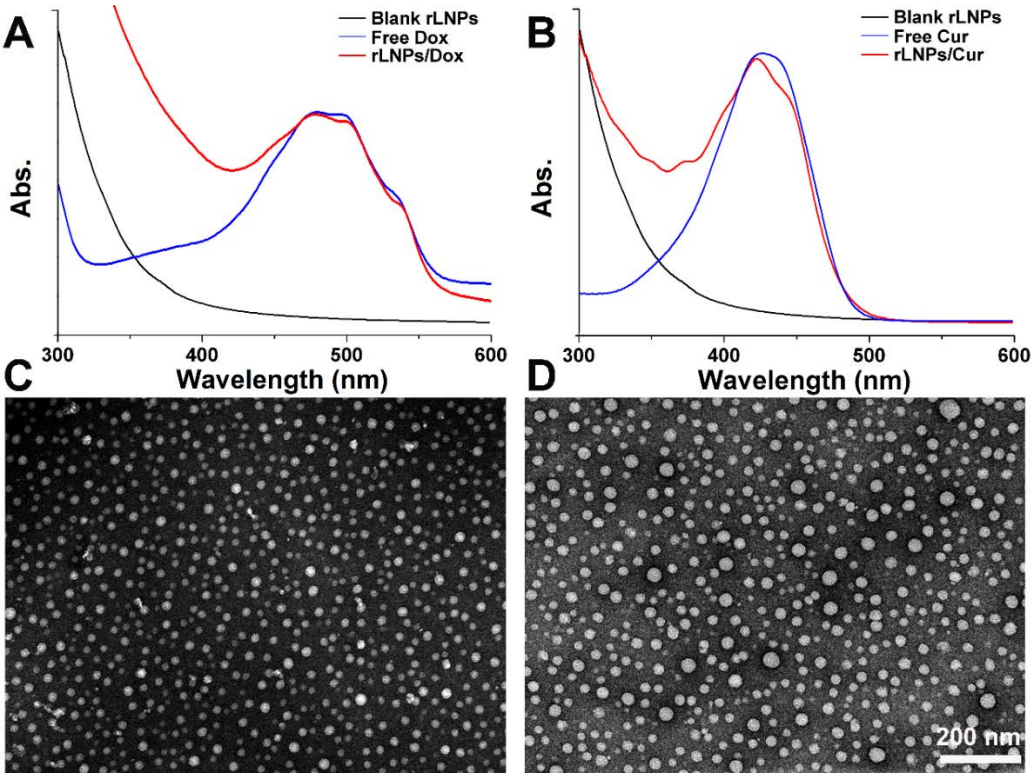

Figure 5. Drug loading of rLNPs. (A and B) UV–vis spectra of blank rLNPs, free drugs and drug-loaded rLNPs. The morphology of rLNPs/Dox (C) and rLNPs/Cur (D). Scale bar: 200 nm.

3.6. The rLNPs/Dox showed promising in vitro and in vivo anticancer performance

Finally, rLNPs/Dox as the model DDS were used for the inhibition of 4T1 cancer cells and the treatment of orthotopic 4T1 tumors. The *in vitro* anticancer performance was first assessed using 4T1 cells. Free Dox and rLNPs/Dox were incubated with 4T1 cells for 24 h, and the cell viability was tested to determine the cytotoxicity of different formulations. As shown in Figure 6A, under all given concentrations, rLNPs/Dox showed comparable inhibition of 4T1 cells to free Dox. Previous studies suggested that LNPs usually show excellent transmembrane and cellular internalization abilities, possibly due to the high affinity between their lipid components and the lipid bilayer of cells. [37, 38] Therefore, it was inferred that rLNPs/Dox can be readily taken up by 4T1 cells and effectively release their loaded cargo to fully realize the anticancer function of Dox.

In addition, an *in vitro* assay was also performed using MCTS, a 3D cell cluster, to mimic the anticancer performance of free Dox and rLNP/Dox on solid tumors. As shown in Figure 6B by MTT assay, free Dox showed inferior inhibition of MCTS compared to rLNPs/Dox. It was previously reported that ultrasmall DDSs usually have better penetration into deep tumor tissue. [39] Moreover, nanoscale DDSs have also been demonstrated to potentiate drug penetration within tumors via other mechanisms, including neighboring effects [40] and transcytosis. [41] These effects are thought to collectively enhance the penetration of rLNPs/Dox into MCTS for potentially stronger inhibition of 3D structured tumors.

Preprints (www.preprints.org) | NOT PEER-REVIEWED | Posted: 3 November 2022 doi:10.20944/preprints202211.0069.v1

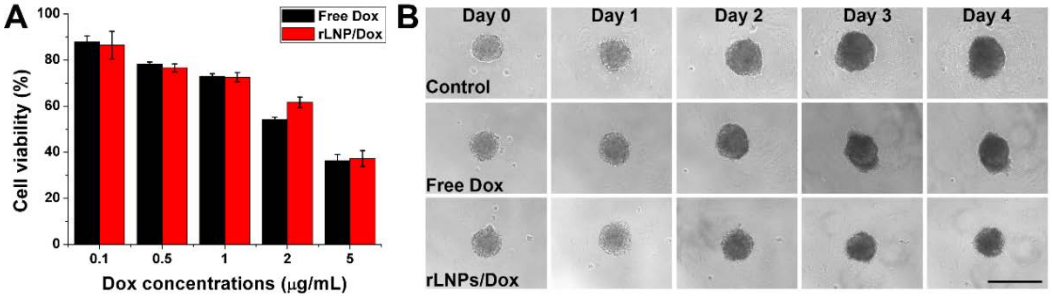

Figure 6. The *in vitro* anticancer performance of rLNPs/Dox. (A) The concentration-dependent cytotoxicity of free Dox and rLNPs/Dox on 4T1 cells after 24 h of incubation. Data are shown as the mean values and standard deviations of three independent results. (B) Image of MCTS after incubation with free Dox or rLNPs/Dox (Dox concentration: 1 μg/mL) for 4 days. Scale bar: 500 μm.

The *in vivo* anticancer studies were performed using orthotopic 4T1 tumor-bearing mice as a model. The tumor volume variations were recorded during a 14-day therapeutic period to reflect the anticancer performance of different formulations. As shown in Figure 7A, compared with the control group, free Dox as the first-line chemotherapeutic drug significantly inhibited the growth of tumors. However, due to its short half-life, free Dox usually show poor accumulation to the tumor tissue, which significantly impair its anticancer performance. [42] In contrast, in line with previous report, rLNPs/Dox showed much more improved anticancer benefits than free Dox, which might ascribe to its preferable accumulation and retention within the tumor tissue. [43] The HE and Ki67 staining shown in Figure 7B support this conclusion. Compared with control and free Dox, rLNPs/Dox-treated tumor tissues showed the highest level of tumor regression (HE) with the lowest level of cell proliferation (Ki67). Both *in vitro* and *in vivo* results provided solid evidence to prove the suitability of rLNPs as drug delivery carriers for cancer treatments.

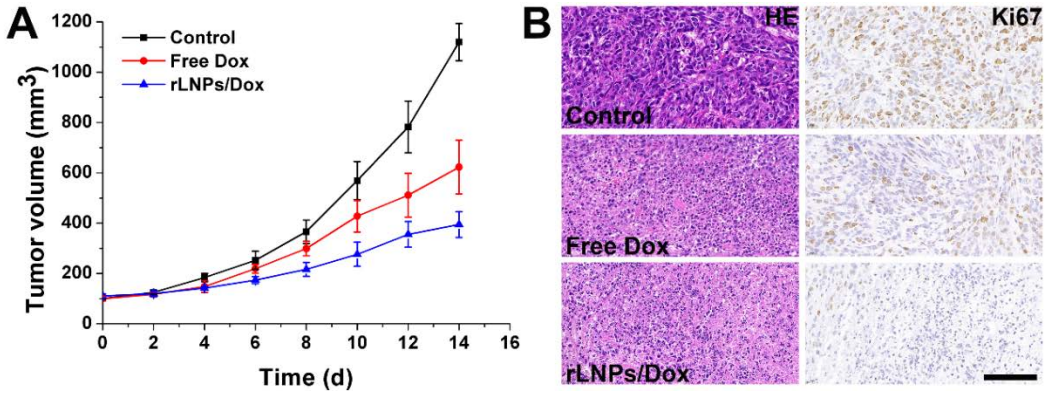

Figure 7. The *in vivo* anticancer performance of rLNPs/Dox. (A) The tumor volume variations and (B) representative images of *ex vivo* tumor sections after HE and Ki67 staining. Scale bar: 100 μm.

4. Conclusion

In summary, in this study, the author proposed the concept and preparation of rLNPs and demonstrated their potential as versatile drug delivery carriers. Their advantages include the following: 1) High reproducibility in preparation from both cells and tissues; 2) Flexible labeling with fluorescent molecules and modifications of targeting ligands and possibly other functional moieties; 3) High biocompatibility; 4) Capable of loading with a variety of drugs; and 5) Good *in vitro* and *in vivo* anticancer performance as a drug carrier and this might be further extended for the treatment of other diseases by loading other kinds of drugs. In the future work, the author will focuses on the following aspects: 1) Extends the applications of rLNPs to different drugs and other disease models; 2) Explores whether there is a cell/tissue specific function of rLNPs; 3) Elucidates whether cell/tissue

 doi:10.20944/preprints202211.0069.v1

education can be realized using rLNPs since they contain the lipidomics of the parent cell/tissue.

Conflict of interest

The author declares no conflict of interest.

Acknowledgment

Our project was supported by the funding from Science Foundation of Jiangsu Province (No. BK20210851); China Postdoctoral Science Foundation Funded Project (No. 2021M690482); Jiangsu Postdoctoral Science Foundation Funded Project (No. 2021K014A); Project of Jiangsu Province Key Laboratory of Radiation Medicine and Protection, Soochow University (No. KJS2104); Science &Technology Support Program of Changzhou (Application Basic Research, No. CJ20210142); Scientific Research Foundation of Jiangsu Provincial Education Department, China (No. 21KJD350003). The author acknowledges the particle distribution data provided by Dr. Qi Jiang of Zhejiang University; the tissue slide preparation, staining, and imaging services provided by Record Biological Technology Co., Ltd. (Shanghai, China); the TEM imaging provided by Zhenjiang ZhuanBo Detection Technology Co., Ltd., and facilities for animal experiments provided by Cavens animal center (Changzhou, China).

References

[1] D.J. Irvine, E.L. Dane, Enhancing cancer immunotherapy with nanomedicine, Nature Reviews Immunology 20(5) (2020) 321-334.
[2] B.Y.S. Kim, J.T. Rutka, W.C.W. Chan, Nanomedicine, New England Journal of Medicine 363(25) (2010) 2434-2443.
[3] J. Nam, S. Son, K.S. Park, W. Zou, L.D. Shea, J.J. Moon, Cancer nanomedicine for combination cancer immunotherapy, Nature Reviews Materials 4(6) (2019) 398-414.
[4] C. Zhang, L. Yan, X. Wang, S. Zhu, C. Chen, Z. Gu, Y. Zhao, Progress, challenges, and future of nanomedicine, Nano Today 35 (2020) 101008.
[5] H.S. Nalwa, A special issue on reviews in nanomedicine, drug delivery and vaccine development, Journal of Biomedical Nanotechnology 10(9) (2014) 1635-1640.
[6] K. Riehemann, S.W. Schneider, T.A. Luger, B. Godin, M. Ferrari, H. Fuchs, Nanomedicine—Challenge and Perspectives, Angewandte Chemie International Edition 48(5) (2009) 872-897.
[7] S. Tao, F. Yu, Y. Song, W. Zhou, J. Lv, R. Zhao, C. Wang, F. Hu, H. Yuan, Water/pH dual responsive in situ calcium supplement collaborates simvastatin for osteoblast promotion mediated osteoporosis therapy via oral medication, Journal of Controlled Release 329 (2021) 121-135.
[8] X. Zhao, Q. Chen, W. Liu, Y. Li, H. Tang, X. Liu, X. Yang, Codelivery of doxorubicin and curcumin with lipid nanoparticles results in improved efficacy of chemotherapy in liver cancer, International journal of nanomedicine 10 (2015) 257.
[9] X. Zhao, R. Shen, L. Bao, C. Wang, H. Yuan, Chitosan derived glycolipid nanoparticles for magnetic resonance imaging guided photodynamic therapy of cancer, Carbohydrate Polymers 245 (2020) 116509.
[10] B. Pelaz, C. Alexiou, R.A. Alvarez-Puebla, F. Alves, A.M. Andrews, S. Ashraf, L.P. Balogh, L. Ballerini, A. Bestetti, C. Brendel, Diverse applications of nanomedicine, ACS nano 11(3) (2017) 2313-2381.
[11] S. Bamrungsap, Z. Zhao, T. Chen, L. Wang, C. Li, T. Fu, W. Tan, Nanotechnology in therapeutics: a focus on nanoparticles as a drug delivery system, Nanomedicine 7(8) (2012) 1253-1271.
[12] E. Beltrán-Gracia, A. López-Camacho, I. Higuera-Ciapara, J.B. Velázquez-Fernández, A.A. Vallejo-Cardona, Nanomedicine review: Clinical developments in liposomal applications, Cancer Nanotechnology 10(1) (2019) 1-40.
[13] H. Cabral, K. Miyata, K. Osada, K. Kataoka, Block copolymer micelles in nanomedicine applications, Chemical reviews 118(14) (2018) 6844-6892.
[14] H. Zhang, Erythrocytes in nanomedicine: An optimal blend of natural and synthetic materials, Biomaterials science 4(7) (2016) 1024-1031.
[15] N.E. Eleraky, A. Allam, S.B. Hassan, M.M. Omar, Nanomedicine fight against antibacterial resistance: an overview of the recent pharmaceutical innovations, Pharmaceutics 12(2) (2020) 142.
[16] L.-P. Wu, D. Wang, Z. Li, Grand challenges in nanomedicine, Materials Science and Engineering: C 106 (2020) 110302.
[17] I. de Lázaro, D.J. Mooney, Obstacles and opportunities in a forward vision for cancer nanomedicine, Nature materials 20(11) (2021) 1469-1479.
[18] N. Arrighetti, C. Corbo, M. Evangelopoulos, A. Pastò, V. Zuco, E. Tasciotti, Exosome-like nanovectors for drug delivery in cancer, Current medicinal chemistry 26(33) (2019) 6132-6148.

 doi:10.20944/preprints202211.0069.v1

[19] Y.-Z. Zhao, B.-X. Shen, X.-Z. Li, M.-Q. Tong, P.-P. Xue, R. Chen, Q. Yao, B. Chen, J. Xiao, H.-L. Xu, Tumor cellular membrane camouflaged liposomes as a non-invasive vehicle for genes: specific targeting toward homologous gliomas and traversing the blood–brain barrier, Nanoscale 12(28) (2020) 15473-15494.
[20] G.H. Nam, Y. Choi, G.B. Kim, S. Kim, S.A. Kim, I.S. Kim, Emerging prospects of exosomes for cancer treatment: from conventional therapy to immunotherapy, Advanced Materials 32(51) (2020) 2002440.
[21] M. Zhang, S. Cheng, Y. Jin, N. Zhang, Y. Wang, Membrane engineering of cell membrane biomimetic nanoparticles for nanoscale therapeutics, Clinical and Translational Medicine 11(2) (2021) e292.
[22] R. Tenchov, R. Bird, A.E. Curtze, Q. Zhou, Lipid Nanoparticles— From Liposomes to mRNA Vaccine Delivery, a Landscape of Research Diversity and Advancement, ACS nano 15(11) (2021) 16982-17015.
[23] M. Li, J. Pei, Z. Ma, J. Fu, F. Chen, S. Du, Docetaxel-loaded ultrasmall nanostructured lipid carriers for cancer therapy: in vitro and in vivo evaluation, Cancer Chemotherapy and Pharmacology 85(4) (2020) 731-739.
[24] F.-Q. Hu, S.-P. Jiang, Y.-Z. Du, H. Yuan, Y.-Q. Ye, S. Zeng, Preparation and characterization of stearic acid nanostructured lipid carriers by solvent diffusion method in an aqueous system, Colloids and Surfaces B: Biointerfaces 45(3-4) (2005) 167-173.
[25] D. Witzigmann, P. Uhl, S. Sieber, C. Kaufman, T. Einfalt, K. Schöneweis, P. Grossen, J. Buck, Y. Ni, S.H. Schenk, Optimization-by-design of hepatotropic lipid nanoparticles targeting the sodium-taurocholate cotransporting polypeptide, Elife 8 (2019) e42276.
[26] R. Dal Magro, F. Ornaghi, I. Cambianica, S. Beretta, F. Re, C. Musicanti, R. Rigolio, E. Donzelli, A. Canta, E. Ballarini, ApoE-modified solid lipid nanoparticles: A feasible strategy to cross the blood-brain barrier, Journal of Controlled Release 249 (2017) 103-110.
[27] V. Matyash, G. Liebisch, T.V. Kurzchalia, A. Shevchenko, D. Schwudke, Lipid extraction by methyl-tert-butyl ether for high-throughput lipidomics *^{s⃞}, Journal of Lipid Research 49(5) (2008) 1137-1146.
[28] X. Zhao, D. Tang, T. Yang, C. Wang, Facile preparation of biocompatible nanostructured lipid carrier with ultra-small size as a tumor-penetration delivery system, Colloids and Surfaces B: Biointerfaces 170 (2018) 355-363.
[29] C. Wang, S. Chen, F. Yu, J. Lv, R. Zhao, F. Hu, H. Yuan, Dual-channel theranostic system for quantitative self-indication and low-temperature synergistic therapy of cancer, Small 17(10) (2021) 2007953.
[30] C. Wang, S. Chen, L. Bao, X. Liu, F. Hu, H. Yuan, Size-controlled preparation and behavior study of phospholipid–calcium carbonate hybrid nanoparticles, International Journal of Nanomedicine 15 (2020) 4049.
[31] F.-Q. Hu, S.-P. Jiang, Y.-Z. Du, H. Yuan, Y.-Q. Ye, S. Zeng, Preparation and characteristics of monostearin nanostructured lipid carriers, International journal of pharmaceutics 314(1) (2006) 83-89.
[32] P. Chand, H. Kumar, N. Badduri, N.V. Gupta, V.G. Bettada, S.V. Madhunapantula, S.S. Kesharwani, S. Dey, V. Jain, Design and evaluation of cabazitaxel loaded NLCs against breast cancer cell lines, Colloids and Surfaces B: Biointerfaces 199 (2021) 111535.
[33] Y. Chen, X. Feng, Y. Zhao, X. Zhao, X. Zhang, Mussel-Inspired Polydopamine Coating Enhances the Intracutaneous Drug Delivery from Nanostructured Lipid Carriers Dependently on a Follicular Pathway, Molecular Pharmaceutics 17(4) (2020) 1215-1225.
[34] B. Tang, Y. Peng, Q. Yue, Y. Pu, R. Li, Y. Zhao, L. Hai, L. Guo, Y. Wu, Design, preparation and evaluation of different branched biotin modified liposomes for targeting breast cancer, European Journal of Medicinal Chemistry 193 (2020) 112204.
[35] V. Mishra, K.K. Bansal, A. Verma, N. Yadav, S. Thakur, K. Sudhakar, J.M. Rosenholm, Solid lipid nanoparticles: Emerging colloidal nano drug delivery systems, Pharmaceutics 10(4) (2018) 191.
[36] R.S. Fernandes, J.O. Silva, L.O.F. Monteiro, E.A. Leite, G.D. Cassali, D. Rubello, V.N. Cardoso, L.A.M. Ferreira, M.C. Oliveira, A.L.B. de Barros, Doxorubicin-loaded nanocarriers: A comparative study of liposome and nanostructured lipid carrier as alternatives for cancer therapy, Biomedicine & Pharmacotherapy 84 (2016) 252-257.
[37] S.Q. Chen, C. Wang, S. Tao, Y.X. Wang, F.Q. Hu, H. Yuan, Rational Design of Redox-Responsive and P-gp-Inhibitory Lipid Nanoparticles with High Entrapment of Paclitaxel for Tumor Therapy, Advanced Healthcare Materials 7(17) (2018) 1800485.
[38] J. Li, B. Chen, T. Yu, M. Guo, S. Zhao, Y. Zhang, C. Jin, X. Peng, J. Zeng, J. Yang, An efficient controlled release strategy for hypertension therapy: Folate-mediated lipid nanoparticles for oral peptide delivery, Pharmacological Research 157 (2020) 104796.
[39] L. Zhu, D. Gao, L. Xie, Y. Dai, Q. Zhao, NIR II-excited and pH-responsive ultrasmall nanoplatform for deep optical tissue and drug delivery penetration and effective cancer chemophototherapy, Molecular Pharmaceutics 17(10) (2020) 3720-3729.
[40] C. Wang, S. Chen, Y. Wang, X. Liu, F. Hu, J. Sun, H. Yuan, Lipase-triggered water-responsive “Pandora's Box” for cancer therapy: Toward induced neighboring effect and enhanced drug penetration, Advanced Materials 30(14) (2018) 1706407.
[41] Y. Liu, Y. Huo, L. Yao, Y. Xu, F. Meng, H. Li, K. Sun, G. Zhou, D.S. Kohane, K. Tao, Transcytosis of nanomedicine for tumor penetration, Nano Letters 19(11) (2019) 8010-8020.
[42] H. Zhang, P. Cui, Z. Gao, S. Zhou, C. Wang, P. Jiang, X. Ni, J. Wang, L. Qiu, A Facile Way To Improve the Bioavailability of Nanomedicine Based on the Threshold Theory, Molecular Pharmaceutics 19(5) (2022) 1647-1655.
[43] J.-b. Du, Y. Cheng, Z.-h. Teng, M.-l. Huan, M. Liu, H. Cui, B.-l. Zhang, S.-y. Zhou, pH-triggered surface charge reversed nanoparticle with active targeting to enhance the antitumor activity of doxorubicin, Molecular Pharmaceutics 13(5) (2016) 1711-1722.